International Journal of Scientific Research in Modern Science and Technology
ISSN: 2583 -7605 (Online)
© IJSRMST | Vol. 4 | Issue 9 | September 2025
Available online at: https://ijsrmst.com/
DOI: https://doi.org/10.59828/ijsrmst.v4i9.367

Analysis of Soret and Dufour Effects on Buoyancy driven MHD Heat Mass Transfer Couette Flow under the Influence of Ramped and Isothermal Temperature settings

F. Abdullahi[1], M.A. Sani[1] and M. Mansur[2]

[1]Department of Mathematics Waziri Umaru Federal Polytechnic Birnin Kebbi, Nigeria

[2]Department of computer Science Waziri Umaru Federal Polytechnic Birnin Kebbi, Nigeria

Corresponding author's E-mail: farukabdullahi@wufpbk.edu.ng

ABSTRACT

This analysis investigates the impact of soret and dufour on MHD heat and mass transfer coquette flow considering the ramped and isothermal conditions due to contributory effects of buoyancy. The analysis has been able to change the governing partial differential equations and their initial and boundary conditions into dimensionless form using the appropriate dimensional variables. Finite element method was employed in finding the solution of dimensionless partial differential equations subject to their initial and boundary conditions. The results from the finding indicates that, velocity profile is enhanced due to the rise in Eckert number (E_c), Buoayancy parameter (r_t), Dufour number (D_f), Solutal Grashof number (G_c), Thermal grashof number (G_r) and Radiation parameter (R) while opposite trends is observed with rise in Jeffery fluid parameter (β). The fluid temperature upsurges due to intensification of G_r, r_t, R, D_f and E_c and shrinks with increase in Prandtl number (P_r). On the other hand there is declining in concentration profile as Schmidt number (S_c) and chemical reaction parameter (K_r) increases, while opposite behavior is seen with Soret number (S_r). Additionally, There is slight boost on skin friction (τ) as r_t and D_f gets increased. Conversely, Nusselt number (N_u) get lowered as D_f increases. Also, N_u and Sherwood number (S_h) enlarges as r_t increases. Furthermore, τ. S_h and N_u gets reduces slightly due to rise in S_r. Finally, the overall results are in complete agreement with the existing literature thereby validating the accuracy and reliability of the present study.

Keywords: *Dufour, Buoyancy, Soret, Ramped Temperature, Isothermal Temperature.*

Nomenclature

E_c	Eckert Number	C_w	Wall Dimensional Concentration
S_r	Soret Number	C_∞	Ambient Concentration
P_r	Prandlt Number	C^*	Dimensional Concentration
T^*	Temperature of the Fluid Close the Plate	g	Accelerature Due to Gravity
T^*	Dimensional Time	C^*_∞	Ambient Fluid Concentration
D_f	Dufour Number	S_C	Schmidt Number
R	Radiation Parameter	G_r	Thermal Grashof Number
M	Magetic Field Parameter	T^*_∞	Ambient Fluid Temperature
u^*	Dimensional Velocity	v	Kinematic Viscosity
τ	Skin Friction	u	Non-Dimensional Velocity
N_u	Nusselt Number	r_t	Buoyancy Parameter
ρ^*	Coefficiennt of Species Expansion	K_r	Chemical Reaction Parameter
θ^*	Dimensional Temperature	β	Jeffery Fluid Parameter
T	Dimensionless Time	M	Hall Current Parameter
C^*	Specific Concentration Near the Plate	G_c	Solutal Grashof Number

1. Introduction.

The soret effect is generally described as the movement of particles (mass flow) produced by temperature gradient and it also called thermo-diffusion while on the other hand the dufour effect is the heat flow produced by the concentration gradient and it is also referred to as diffusion thermo. These two important quantities have significant role in what is called double diffusive transport system especially in fluid with light and moderate molecular weight. These two quantities effects play a vital role in understanding and optimization of fluid with significant temperature and concentration gradients which includes chemical engineering processes, hydro and geophysical system manufacturing of photochemical insulation of materials and nuclear waste disposal. Several research works have been conducted by many researchers on these two important quantities.

The study of MHD viscous dissipation ohmic heating in porous medium under the influence of heat source and chemical reaction was analyzed by [1]. Likewise [2] showed that velocity enhances due to to rise in dufour number. This was stated in their study on MHD buoyancy and Maxwell-nano effects in the presence of soret and dufour. The revelation of soret number improves velocity profile was reported by [3]. The investigation of coquette flow with buoyancy effect due to onset of soret was carried out by [4]. The examination of MHD micro-polar fluid in the presence of soret and dufour over vertical riga plate was conducted by [5]. Anlysis of soret and dufour MHD in past permeable sheet due to viscous dissipation and chemical reaction was carried out by [6]. The study of MHD heat mass transfer in the presence of soret and thermal radiation was investigated by [7]. The analysis of MHD heat transfer due to generation and radiation

was conducted by [8]. Also, [9] carried out study on casson fluid MHDin accelerated plate in the presence of soret as a result of constant caputo fractional derivative. Dufour enhances concentration, the was reported in the study of [10] on MHD casson fluid in porous medium in the presence of thermo-diffusion. The investigation of MHD free convective flow due to enthalpy generation in coaxial cylinder with non-linear thermal radiation was conducted by [11].

Furthermore, [12] revealed that velocity gets increased due to rise in hall current in their reseach on MHD two ionized fluid flow. Likewise, [13] carried out study on MHD Jeffery fluid with heat absorption in a vertical porous medium. The analysis of MHD heat mass transfer in an inclined porous plate was carried out by [14] and showed that temperature gets high due to surface inclined angle increase. From analysis of [15] on MHD heat mass treansfer with two ionized fluid, it reported that hall-current enhances velocity profile. The influence of MHD casso-Nano-fluid with hall-current and non-linear thermal radiation over a vertical extending sheet was analyzed by [16]. The analysis of MHD heat transfer model on parameter estimation space was conducted by [17]. The study of MHD fluid radiative absorption medium in the presence of hall-current was examined by [18]. From study of [19] velocity gets increased due rise in buoyancy this was stated in their analysis on MHD heat mass transfer due to buoyancy and hall-current effects. [20]–[22] carried out examination on MHD heat mass transfer flow and stated hall-current has improving effects on velocity profile. The impact of thermophoresis and Brownian motion on MHD boundary layer was investigated by [23]

The present study is an extension of [24] model in which the influence of MHD Jeffery fluid heat mass transfer in the presence of chemical reaction and ramped temperature was analyzed. This study tends to build up upon this model by investigation the combined impact of soret and dufour subject to Ramped and isothermal temperature in the presence of buoyancy distribution impact.. The outcome of this research is expected to have practical applications in chemical engineering processes, hydro and geophysical system, manufacturing of photochemical insulation of materials and nuclear waste disposal.

2. Formulation of the Problem

Consider an unsteady (MHD) free convection flow of an incompressible, electrically conducting fluid past an infinite vertical plate.

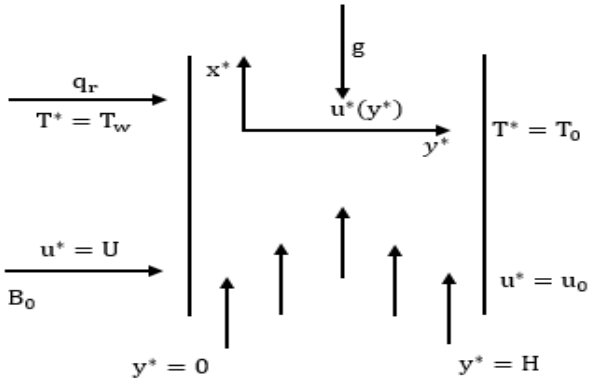

Figure1: Geometry of Flow

Let x*-axis be taken upward vertically along infinite vertical plate and for normal to the plate we let y*-axis. Transversely normal to the plate there is uniform magnetic field with strength H_0. As a result assumption of a very low magnetic Reynolds causing its insignificant effects number then induced magnetic field is neglected. Temperature of the plate and that of surrounding are assumed to be equal at the beginning. Initially, the temperature of the plate T^* and the surrounding T_w^*. Additionally, concentration species are presumed to be equal to that ambient fluid C_w^* and C_0^*. At time t*>0, the plate raised abruptly new temperature value T_w^* which results the development current convection in the fluid adjacent to the plate. Simultaneously, to plate surface there is constant rate of mass introduction, under Boussineq approximation the problem is governed by the following non-linear partial differential equations:

$$\frac{\partial u^*}{\partial t^*} = \left(\frac{1}{1+\beta}\right)\frac{\partial^2 u^*}{\partial y^{*2}} + g\beta^*(C^* - C_\infty^*) + g\beta^*(T^* - T_\infty^*) - \left(\frac{m}{1+m^2}\right)\frac{\sigma}{\rho}\beta_0^2 u^* \quad (1)$$

$$\frac{\partial T^*}{\partial t^*} = \frac{k}{\rho C_p}\frac{\partial^2 T^*}{\partial y^{*2}} + Ec\left[\frac{du^*}{dy^*}\right]^2 + D_f\frac{\partial^2 C}{\partial y^2} + \frac{(C^* - C_0^*)}{(C_w^* - C_\infty^*)}\frac{\partial T^*}{\partial t^*} + (T^* - T_\infty^*) \quad (2)$$

$$\frac{\partial C^*}{\partial t^*} = D\frac{\partial^2 C^*}{\partial y^{*2}} + S_r\frac{\partial^2 T^*}{\partial y^2} - K_r^*(C^* - C_\infty^*) \quad (3)$$

The dimensionless variables are defined as;

$$t^* > 0\begin{Bmatrix} t^* \le 0:\ u^* = 0, T^* = T_0,\ \varphi^* = C_0 \text{for all } 0 \le y^* \le L \\ u^* = u = \frac{u}{U_0}, T^* = rtT_w^*, \text{at } y^* = 0 \\ u^* = 0, T^* = T_\infty^*, \text{at } y^* = \infty \end{Bmatrix} \quad (4)$$

The governing differential equations are to be made dimensionless by:

$$\begin{Bmatrix} U_0 = (vg\beta\Delta T)^{\frac{1}{3}}, L = \left(\frac{g\beta\Delta T}{v^2}\right)^{\frac{-1}{3}}, T_R = \left(\frac{g\beta\Delta T}{v^{\frac{-1}{3}}}\right)^{\frac{-2}{3}} \\ \Delta T = T_w^* - T_\infty^*, t = \frac{t^*}{T_R}, y = \frac{y^*}{L} \\ u = \frac{u^*}{U_0}, K = \frac{K^*}{vT_R}, \theta = \frac{T^* - T_\infty^*}{T_w^* - T_\infty^*}, \varphi = \frac{C^* - C_\infty^*}{C_w^* - C_\infty^*}, D_f = \frac{S_t(C^* - C_0^*)}{\alpha(C_w^* - C_\infty^*)} \\ Pr = \frac{\mu C_\rho}{k}, Ec = \frac{U_0^2}{C_\rho \Delta T}, N = \frac{\beta^*}{\beta(T_w^* - T_\infty^*)}, M = \frac{\sigma\beta_0^2 u}{\rho u^2} \\ R = \frac{16a\sigma^* v^2 T_\infty^*}{u^2 \rho C_p}, K_r = \frac{Kr_0 u}{u^2}, S_c = \frac{v}{D}, G_c = \frac{g\beta^* v(C_w^* - C_\infty^*)}{u^3} \end{Bmatrix} \quad (5)$$

Using equation (5) on (1) to (4) the following dimensionless forms are obtained:

$$\frac{\partial u}{\partial t} = \left(\frac{1}{1+\beta}\right)\frac{\partial^2 u}{\partial y^2} + Gr\theta + G_c\varphi - \left(M + \frac{1}{K}\right)u \quad (6)$$

$$\frac{\partial \theta}{\partial t} = \frac{1}{Pr}\frac{\partial^2 \theta}{\partial y^2} + Ec\left[\frac{du}{dy}\right]^2 + D_f\frac{\partial^2 \theta}{\partial y^2} + R\theta \quad (7)$$

$$\frac{\partial \varphi}{\partial t} = Sc\frac{\partial^2 \varphi}{\partial y^2} + D_f\frac{\partial^2 \varphi}{\partial y^2} - K_r\varphi \quad (8)$$

$$\begin{Bmatrix} t \le 0: u = 0, \theta = 2, \varphi = 0 \text{ for all } y \\ \text{For } t \ge 0: u = \cos w, \theta = rt, \varphi = 1 \text{ at } y = 0 \\ u = 0, \theta \to 0, \text{at } y \to \infty \end{Bmatrix} \quad (9)$$

3. Method of the Solution

Applying the boundary condition (9) to solve (6) to (8) numerically using FEM as:

Over an element $e, y_i \le y \le y_j$ and with application of FEM on (6) to (8) we get:

$$\int_{y_i}^{y_j} N^T \left\{\frac{\partial u}{\partial t} = \left(\frac{1}{1+\beta}\right)\frac{\partial^2 u}{\partial y^2} + Gr\theta + G_c\varphi - \left(M + \frac{1}{K}\right)u\right\} dy = 0 \quad (10)$$

Equation (10) is summarized to

$$\int_{y_i}^{y_j} N^T \left\{M_2 \frac{\partial^2 u}{\partial y^2} - \frac{\partial u}{\partial t} + P - uM_1\right\} dy = 0 \quad (11)$$

$M_2 = \left(\frac{1}{1+\beta}\right)$ and $M_1 = \left(M + \frac{1}{K}\right)$, $P = Gr\theta + G_c\varphi$

Integration by parts is applied on (11) to get:

$$N^T\left[M_2 \frac{\partial u}{\partial t}\right]_{y_i}^{y_j} - \int_{y_i}^{y_j} M_2 \frac{\partial N^T}{\partial y}\frac{\partial u}{\partial y} dy - \int_{y_i}^{y_j} N^T \frac{\partial u}{\partial t} dy - M_1 \int_{y_i}^{y_j} N^T u dy + P\int_{y_i}^{y_j} N^T dy += 0 = 0 \quad (12)$$

The first term of equation (12) is overlooked

$$M_2 \int_{y_i}^{y_j} \frac{\partial N^T}{\partial y}\frac{\partial u}{\partial y} dy + \int_{y_i}^{y_j} N^T \frac{\partial u}{\partial t} dy + M_1 \int_{y_i}^{y_j} N^T u dy - P\int_{y_i}^{y_j} N^T dy += 0 = 0 \quad (13)$$

We now take $u^{(e)} = u_i N_i + u_j N_j \Rightarrow u^{(e)} = [N][u]^T$ be a linear approximation solution over the nodal element e, $y_i \le y \le y_j$ where $u^{(e)} = [u_i, u_j]$ and $N = [N_i, N_j]$ also, u_i and u_j are the velocity component at the i^{th} and j^{th} nodes of the typical element(e) $y_i \le y \le y_j$. Also, N_i and N_j are called basis or (shape) functions and can be defined as: $N_i = \frac{y_j - y}{y_j - y_i}$ and $N_i = \frac{y - y_i}{y_j - y_i}$

Applying the above on (13) we get

$$M_2 \int_{y_i}^{y_j} \begin{bmatrix} N_i'N_i' & N_i'N_j' \\ N_i'N_j' & N_j'N_j' \end{bmatrix} \begin{bmatrix} u_i \\ u_j \end{bmatrix} dy + \int_{y_i}^{y_j} \begin{bmatrix} N_iN_i & N_iN_j \\ N_iN_j & N_jN_j \end{bmatrix} \begin{bmatrix} \dot{u_i} \\ \dot{u_j} \end{bmatrix} dy + M_1 \int_{y_i}^{y_j} \begin{bmatrix} N_iN_i & N_iN_j \\ N_iN_j & N_jN_j \end{bmatrix} dy - P\int_{y_i}^{y_j} \begin{bmatrix} N_i \\ N_j \end{bmatrix} = 0 \quad (14)$$

Equation (14) is simplified to get:

$$\frac{M_2}{l}\begin{bmatrix} 1 & -1 \\ -1 & 1 \end{bmatrix}\begin{bmatrix} u_i \\ u_j \end{bmatrix} + \frac{l}{6}\begin{bmatrix} 2 & 1 \\ 1 & 2 \end{bmatrix}\begin{bmatrix} \dot{u_i} \\ \dot{u_j} \end{bmatrix} + \frac{M_1 l}{6}\begin{bmatrix} 2 & 1 \\ 1 & 2 \end{bmatrix}\begin{bmatrix} u_i \\ u_j \end{bmatrix} - \frac{lP}{2}\begin{bmatrix} 1 \\ 1 \end{bmatrix} = 0 \quad (15)$$

Where $l = y_j - y_i = h$ and prime and dot indicates differentiation with respect to y and t respectively. Now assembling the equations (15) for the two consecutive elements $y_{i-i} \le y \le y_i$ then the following is obtained:

$$\frac{M_2}{l^2}\begin{bmatrix} 1 & -1 & 0 \\ -1 & 2 & -1 \\ 0 & -1 & 1 \end{bmatrix}\begin{bmatrix} u_{i-1} \\ u_i \\ u_{i+1} \end{bmatrix} + \frac{1}{6}\begin{bmatrix} 2 & 1 & 0 \\ 1 & 4 & 1 \\ 0 & 1 & 2 \end{bmatrix}\begin{bmatrix} \dot{u_{i-1}} \\ \dot{u_i} \\ \dot{u_{i+1}} \end{bmatrix} + \frac{M_1}{6}\begin{bmatrix} 1 & -1 & 0 \\ -1 & 2 & -1 \\ 0 & -1 & 1 \end{bmatrix}\begin{bmatrix} u_{i-1} \\ u_i \\ u_{i+1} \end{bmatrix} - \frac{P}{2}\begin{bmatrix} 1 \\ 2 \\ 1 \end{bmatrix} = 0 \quad (16)$$

Now consider the two-row corresponding to the node i to zero with $i = h$, from equation (16) the difference scheme reads:

$$\frac{M_2}{h^2}(-u_{i-1} + 2u_i - u_{i+1}) + \frac{1}{6}(-\dot{u_{i-1}} + 4\dot{u_i} + \dot{u_{i+1}}) + \frac{\dot{M_1}}{6}(\dot{u_{i-1}} + 4\dot{u_i} - \dot{u_{i+1}}) = P \quad (17)$$

Using the trapezoidal rule on (17) the following system of equations in Crank-Nicolson method is obtained as:

$$A_1 u_{i-1}^{n+1} + A_2 u_i^{n+1} + A_3 u_{i-1}^{n} = A_4 u_{i-1}^{n} + A_5 u_i^{n} + A_6 u_{i+1}^{n} + P^* \quad (18)$$

Similarly applying the same method to solve equation (7) and (8) we get

$$B_1 \theta_{i-1}^{n+1} + B_2 \theta_i^{n+1} + B_3 \theta_{i-1}^{n} = B_4 \theta_{i-1}^{n} + B\theta_i^{n} + B_6 \theta_{i+1}^{n} + Q \quad (19)$$

$$C_1 \varphi_{i-1}^{n+1} + C_2 \varphi_i^{n+1} + C_3 \varphi_{i-1}^{n} = C_4 \varphi_{i-1}^{n} + C_5 \varphi_i^{n} + C_6 \varphi_{i+1}^{n} + R^* \quad (20)$$

Where:

$A_1 = 2 - 6M_2 r + rM_1 h^2$, $A_2 = 8 + 12M_2 r + rM_1 h^2$, $A_1 = 2 - 6M_2 r + rM_1 h^2$

$A_4 = 2 + 6M_2 r - rM_1 h^2$, $A_5 = 8 - 12M_2 r - rM_1 h^2$, $A_6 = 2 + 6M_2 r + rM_1 h^2$, $B_1 = Pr - 3r$, $B_2 = 4Pr + 6r$, $B_3 = Pr - 3r$ $B_4 = Pr + 3r$, $B_5 = 4Pr - 6r$, $B_6 = Pr + 3r$

$C_1 = Sc - 3r$, $C_2 = 4Sc + 6r$, $C_3 = Sc - 3r$ $C_4 = Sc + 3r$, $C_5 = 4Sc - 6r$, $C_6 = Sc + 3r$

$$Q = 6rPr\left[Ec\left[\frac{\partial u}{\partial y}\right]^2 - D_f \frac{\partial^2 C}{\partial y^2} - R\theta_i^n\right], \quad P^* = 12rh^2(Gr\theta_i^n + G_c\varphi_i^n), \quad R^* = 6rh^2 ScK_r\varphi_i^n$$

4. Results and Discussions

The present's analysis investigates the impact of soret and dufour on MHD heat and mass transfer coquette flow considering the ramped and isothermal conditions due to contributory effects of buoyancy. The study presented a series of graphical diagrams show the impact of the key governing parameters on velocity, temperature and concentration profile respectively. Moreover there is a numerical table giving highlight on the influence of selected parameters on skin friction, nusselt number and Sherwood number. The parameters and their default values used in this investigations are: buoyancy parameter ($r_t = 0.1$), Eckert number ($E_c = 0.1$), dufour number ($D_f = 0.1$), soret number ($S_r = 0.1$), Jeffery fluid parameter ($\beta = 0.1$), grashof number ($G_r = 1$), solutal grashof number ($G_c = 1$), radiation parameter ($R = 0.1$) and Magnetic parameter ($M = 1$).

For validation of accuracy and reliability of the numerical results obtained in this analysis, a comparative analysis is made in **Figure 2** below: From the diagram comparisons it can be clearly seen that the finding of the present analysis are in good agreement with that of [24] thereby confirming the validity of this analysis.

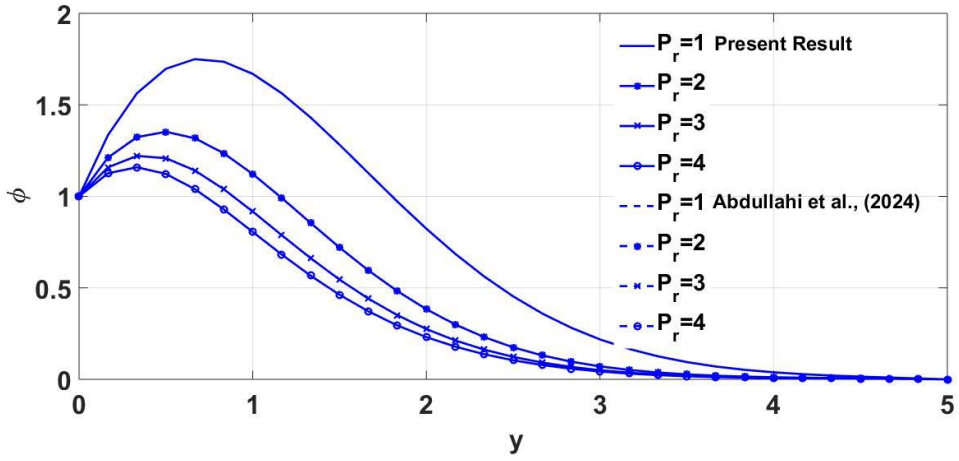

Fig. 2: Comparison between the result of [24] and current results when $S_r = 0, r_t = 0, D_f = 0$

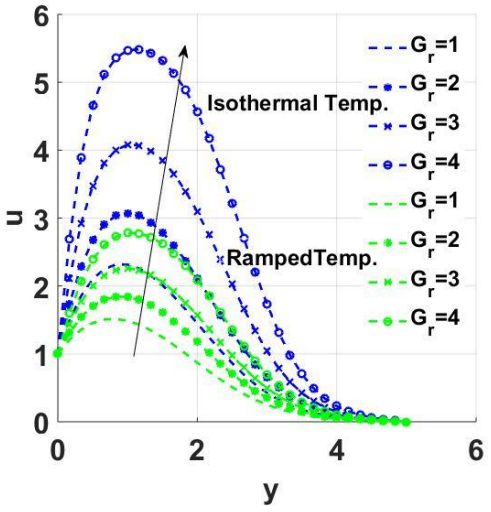

Figure 3: Impact of G_r on u

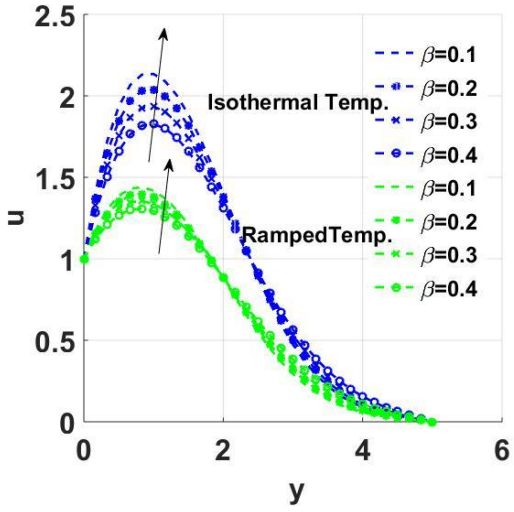

Figure 4: Impact of β on u

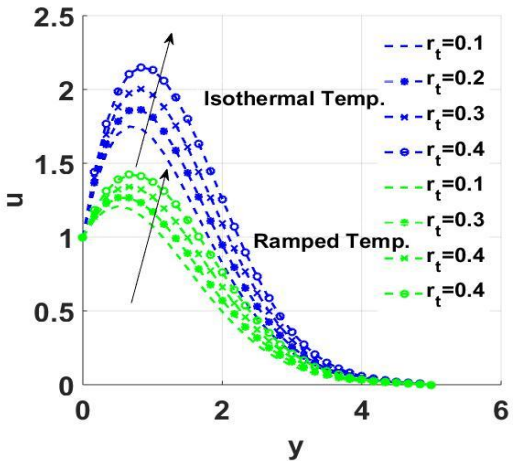

Figure 5: Impact of r_t on u

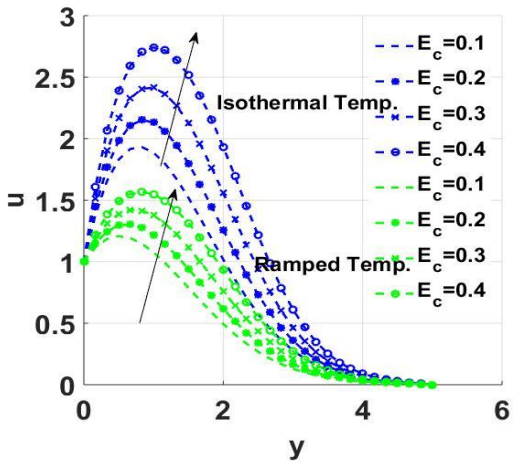

Figure 6: Impact of E_c on u

Figure 3 demonstrates the velocity tends to get high with rise in thermal grash of number (G_r). this increase is a result of buoyancy force ratioss to viscous forces. As G_r rises the effects of buoyancy becomes so intense thereby speedying the fluid flow. In **Figure 4**, reveals that intensification of Jeffery fluid parameter (β)cause lowering the velocity profile. This reduction is as a result additional resistence caused by β which leads to suppress flow intensity and thereby slow down convection motion of the fluid. **Figure 5** shows that the velocity profile experience significant rise as buoyancy parameter (r_t) increases. This rise is a result of significant rise in buoyancy-driven forces in the fluid thereby enhancing its motion. Also, **Figure 6** describes the impact of Eckert number (E_c) on fluid velocity which shows more values of E_c more rise in fluid velocity. This because fluid's kinetic energy is converted to internal energy (enthalpy) which rises thermal activity and hence promotes faster fluid motion.

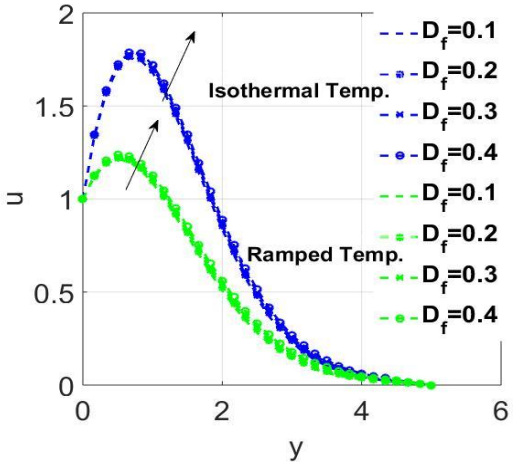

Figure 7: Impact of D_f on u

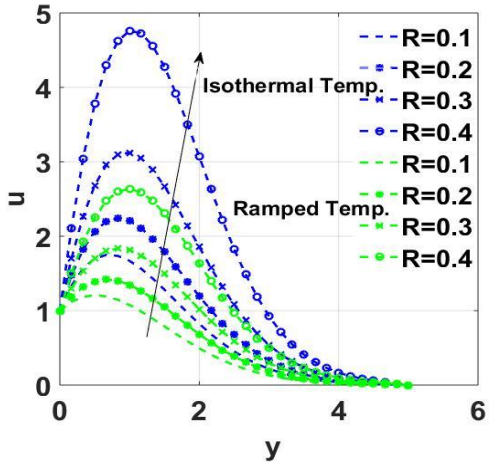

Figure 8: Impact of R on u

Figure 7 describes the characteristics of dufour number (D_f) on velocity profile. From the digram there is slight increase in fluid velocity with the rise in D_f. this rise is attributed to stronger concentration gradients which increase high mass diffusion rate and energy transport among the particles thereby contributing to flow of the fluid. Likewise **figure 8** depicts the action of (R) radiation parameter on velocity profile. From the figure there is intensification of fluid velocity with rise in R. this due to the thickening of thermal boundary layer by the parameter which causes high fluid movement.

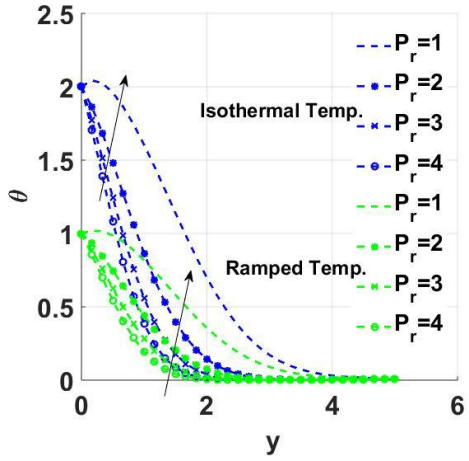

Figure 9: Impact of P_r on θ

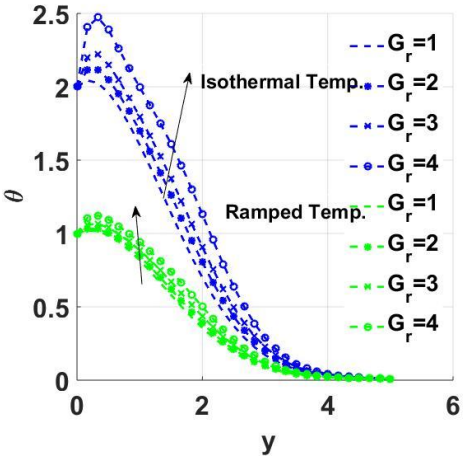

Figure 10: Impact of G_r on θ

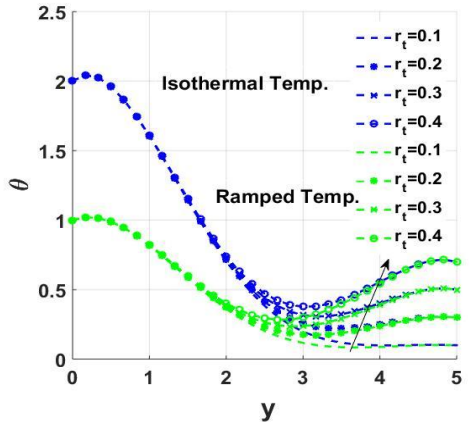

Figure 11: Impact of r_t on θ

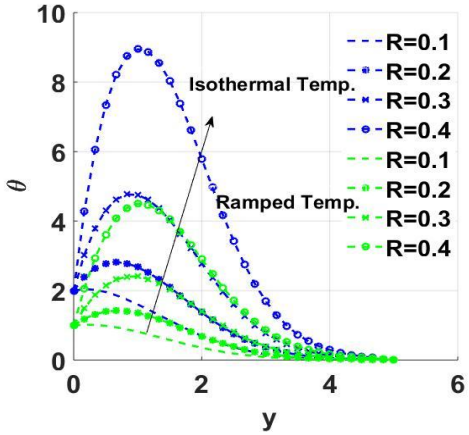

Figure 12: Impact of R on θ

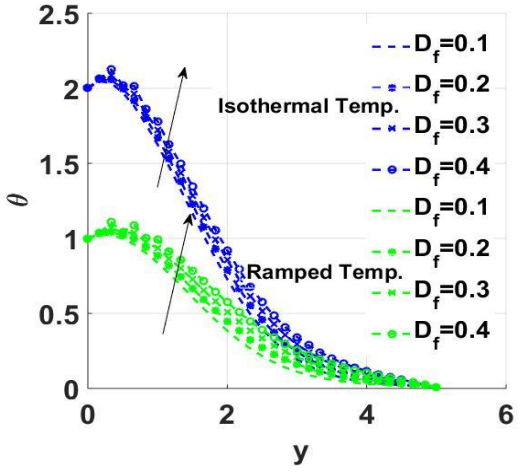

Figure 13: Impact of D_f on θ

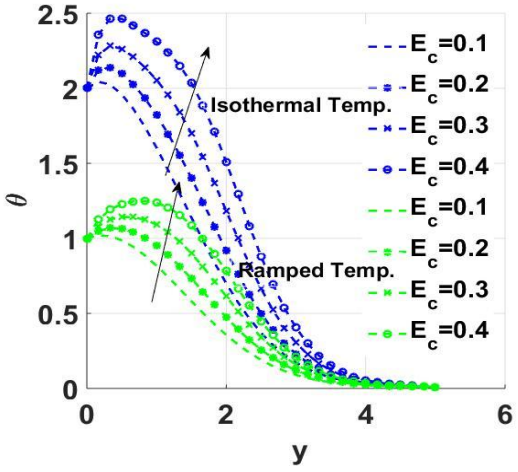

Figure 14: Impact of E_c on θ

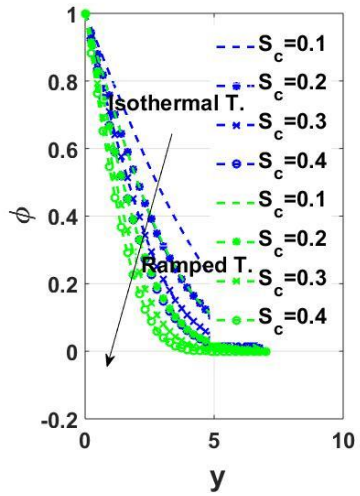

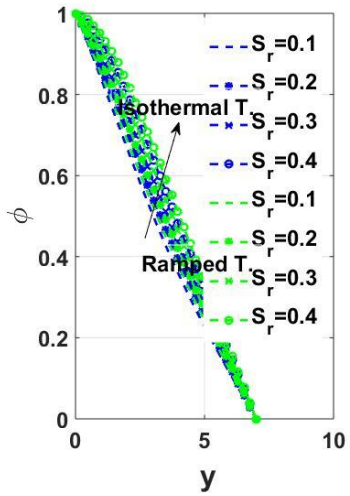

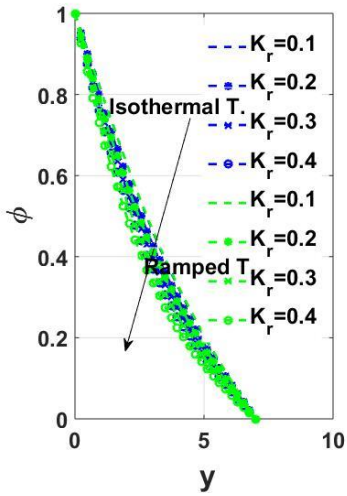

Fig. 15: Impact of S_c on φ **Fig.16:** Impact of S_r on φ **Fig.17:** Impact of K_r on φ

Figure 9 portrays the impact (P_r) on temperature profile. As it is seen from the figure fluid temperature gets diminished with rise in P_r. This diminishing impact is as a result reduction in thermal diffusivity thereby reducing heat conduction rate and subsequently diminishing the fluid temperature. **Figure 10** demonstrates the impact of grashof number (G_r) on fluid temperature. As G_r rises the fluid temperature also rises. This rise is due to enhanced buoyancy forces which facilitate thermal energy effective distribution. The influence of buoyancy parameter (r_t) on fluid temperature is displayed in **Figure 11**. More values of r_t causes noticeable rise in fluid temperature which can be attributed to amplified buoyancy forces in the fluid which enhances greater conductivity and thermal transport. **Figure 12** displays the effects of radiation parameter (R) on fluid temperature. From the figure fluid temperature enlarges due to rise in R. this rise is as a result decrease in absorption coefficient which increases the accumulation of radiative heat flux within the fluid thereby enhancing fluid temperature. The effect of dufuor number (D_f) on temperature profile is depicted in **Figure 13**. From the figure fluid temperature increases with rise in D_f. This because dufour number causes greater thermal conductivity and heat transfer rates. In **Figure 14**, the influence of Eckert number (E_c) is displayed. From the figure there is substantial growth in fluid temperature due to the rise in E_c. This

happens because the action of E_c converts kinetic energy into internal energy and hence promotes fluid thermal energy thereby raising the fluid temperature, **Figure 15** depicts the impact of (S_c) on concentration profile. From the figure the concentration reduces with the increase S_c. The reduction is as a result decrease in mass diffusivity resulting from the high S_c values which restricts spread of and therefore causes thinner concentration. Conversely, there is increase in fluid concentration in **Figure 16** with intensification of Soret number (S_r). This increase as a result of production of thermal gradient which contributes to the rise in concentration profile within the system. Finally, **Figure 16** describes the action of (K_r) on concentration profile. It evident that fluid concentration gets lowered with the rise in K_r. This happens as elevated rate of reaction increase faster molecules interaction and consumption of species thereby lowering level of concentration.

Table 1: Impact of D_f, r_t and S_r on τ, N_u, and S_h

D_f	τ	N_u	S_h	r_t	τ	N_u	S_h	S_r	τ	N_u	S_h
0.1	0.0385	0.1761	0.0977	0.1	0.0277	0.0903	0.0921	0.1	0.0278	0.1768	0.0977
0.2	0.0510	0.1750	0.0977	0.2	0.1869	0.0910	0.0969	0.2	0.0277	0.1335	0.0949
0.3	0.0629	0.1741	0.0977	0.3	0.5113	0.0916	0.106	0.3	0.0277	0.0903	0.0921

Tables 1 display the impact of dufour number (D_f), buoyancy parameter (r_t) and Soret number (S_r) on skin friction (τ), Nusselt number (N_u) and Sherwood number (S_h). From the table there is slight enhancement on τ as r_t and D_f gets increased. This enhancement is due to of significant rise in buoyancy-driven forces in the fluid thereby enhancing its motion. Conversely, N_u get lowered as D_f increases. Also, N_u and S_h enlarges as r_t increases. Finally, S_h and N_u gets reduces due to rise in S_r

5. Conclusion

This analysis investigates the impact of soret and dufour on MHD heat and mass transfer coquette flow considering the ramped and isothermal conditions due to contributory effects of buoyancy. Finite element method was employed to numerically find the solution of governing partial differential equations. **The summary of the main findings are as follows:**

i. The fluid velocity gets enhanced with rise in Eckert number (E_c), buoyancy parameter (r_t), sulutal grashof number (C_c), dufour number (D_f), thermal grashof number (G_r) and radiation parameter (R). Conversely, the fluid velocity gets reduced with rise in Jeffery fluid parameter (β).

ii. Similarly the fluid temperature gets improved with rise in: E_c, D_f, R, r_t, and G_r. Conversely, it gets reduceddue to rise in P_r

iii. The fluid concentration improves with increase in soret number S_r and decreases due to rise in Schmidt number (S_c) and chemical reaction parameter (K_r).

iv. There is slight enhancement on τ as r_t and D_f gets increased. Conversely, N_u get lowered as D_f increases. Also, N_u and S_h enlarges as r_t increases. Finally, τ. S_h and N_u gets reduces due to rise in S_r

.

CONFLICT OF INETREST

There is no conflict of interest as all authors have approved this submission.

References

[1] B. K. Taid and N. Ahmed, "MHD Free Convection Flow Across an Inclined Porous Plate in the Presence of Heat Source , Soret Effect , and Chemical Reaction Affected by Viscous Dissipation Ohmic Heating," vol. 12, no. 5, pp. 6280–6296, 2022, doi: https://doi.org/10.33263/BRIAC125.62806296 MHD.

[2] B. Y. Isah and F. Abdullah, "Unsteady MHD Heat Mass Transfer Couette Flow in a Free Convective Vertical Channel due to Dufour and Buoyancy Distribution Effects," vol. 3, no. 4, pp. 104–120, 2021, doi: https://doi.org/10.37933/nipes.e/3.4.2021.12.

[3] M. Nanofluid, T. Emission, M. Williams, and I. B. Yabo, "The Upshots of Dufour and Soret in Stretching Porous Flow of Convective The Upshots of Dufour and Soret in Stretching Porous Flow of Convective Maxwell Nanofluid with Nonlinear Thermal Emission," no. October, pp. 37–50, 2024, doi: 10.11648/j.ijtam.20241003.12.

[4] B. Y. Isah and F. Abdullah, "Buoyancy Reaction on Unsteady MHD Couette Flow in Free Convective Vertical Channels Due to Onset of Soret Effect," vol. 2, pp. 34–50, 2020, doi: https://doi.org/10.37933/nipes.e/2.2020.4.

[5] K. Borah, J. Konch, and S. Chakraborty, "Soret and dufour effects on mhd flow of a micropolar fluid past over a vertical riga plate," vol. 22, no. 1, pp. 5–18, 2023, doi: 10.17512/jamcm.2023.3.01.

[6] B. R. J. and K. V. V. Kayalvizhi M., Indumathi N., Renuka P., "Dufour, Soret and Dissipation Effects on Magnetohydrodynamic Flow past a Stretching Permeable Sheet with Radiative Chemical Reaction and Heat Source," vol. 12, no. 10, pp. 217–229, 2024, doi: 10.21474/IJAR01/19634.

[7] K. Raghunath, "Study of Heat and Mass Transfer of an Unsteady Magnetohydrodynamic (MHD) Nanofluid Flow Past," vol. 12, no. 3, pp. 767–776, 2023, doi: 10.1166/jon.2023.1965.

[8] M. Akter and M. Hossain, "Heliyon Heat generation and radiative effects on time-dependent free MHD convective transport over a vertical permeable sheet," *Heliyon*, vol. 9, no. 10, pp. 1–14, 2023, doi: 10.1016/j.heliyon.2023.e20865.

[9] S. Abbas *et al.*, "Soret Effect on MHD Casson Fluid over an Accelerated Plate with the Help of Constant Proportional Caputo Fractional Derivative," 2024, doi: 10.1021/acsomega.3c07311.

[10] N. L. Ramesh, P. A. Dinesh, and B. V Shilpa, "Effect of Diffusion-Thermal on Mixed Convective Casson Fluid flow in a Porous Channel," vol. 71, no. 10, pp. 1526–1536, 2023, doi: 10.18311/jmmf/2023/35811.

[11] M. Isah, B Y, abubakarr , Z D, Usman, H, Mamuda, “Analysis of Entropy Generation Within Coaxial Cylinder on MHD Free Convective Flow Due to Nonlinear Thermal Radiation in an Isothermal / Isoflux Condition,” no. January, 2025, doi: 10.1002/htj.23269.

[12] T. L. Raju and V. G. Rao, “Effect of Hall Currents on Unsteady Magnetohydrodynamic two-Ionized Fluid Flow and Heat Transfer in a Channel,” Vol. 26, no. 2, pp. 84–106, 2021, doi: 10.2478/ijame-2021-0021.

[13] S. Saleh, L. Jabaka, and F. Sani, “Heat Absorption and Magneto hydro dynamic (MHD) Effects on Jeffery Fluid Flow past a Vertical Porous Plate with Variable Suction,” vol. 4, no. 12, pp. 56–62, 2022, doi: 10.35629/5252-04125662.

[14] L. Mogirango and I. Chepkwony, “Heat and Mass Transfer in MHD Flow about an Inclined Porous Plate,” vol. 25, no. 4, pp. 106–115, 2023, doi: 10.9734/JERR/2023/v25i4906.

[15] T. L. R. Rao, V Gowri Sankara, “The influence of Hall Currents on Unsteady-MHD Heat Transfer Flow in a Conducting Channel Containing Two Ionized Fluids,” vol. 29, no. 3, pp. 118–149, 2024, doi: 10.59441/ijame/187212.

[16] W. Demis, G. Awgichew, and E. Haile, “Mixed Convection Flow of MHD Casson Nanofluid over a Vertically Extending Sheet with Effects of Hall , Ion Slip and Nonlinear Thermal Radiation Mixed Convection Flow of MHD Casson Nanofluid over a Vertically Extending Sheet with Effects of Hall , Ion Slip,” vol. 23, no. 2024, 2024, doi: 10.1016/j.ijft.2024.100762.

[17] Y. Liu, X. Jiang, and J. Jia, “Numerical Simulation and Parameter Estimation of the Space-Fractional Magnetohydrodynamic Flow and Heat Transfer Coupled Model,” *fractal Fract. Artic.*, vol. 8, no. 557, 2024, doi: https://doi.org/ 10.3390/fractalfract8100557.

[18] S. Rana, K. Mahmud, R. Mehmood, and M. M. Bhatti, “Oblique Flow of Shear Thinning Fluid through an Absorptive Radiative Medium with Hall Effect,” vol. 2023, no. 4, pp. 1–16, 2023, doi: https://doi.org/10.1155/2023/3210794 Research.

[19] F. Abdullahi, I. H. Wala, M. A. Sani, and M. M. Sani, “Influence of Hall Current and Buoyancy Distribution on MHD Time Dependent Heat Mass Transfer,” vol. 4, no. 1, pp. 97–110, 2022.

[20] H. Ullah *et al.*, “Neuro-Computing for Hall Current and MHD Effects on the Flow of Micro-Polar Nano-Fluid Between Two Parallel Rotating Plates,” *Arab. J. Sci. Eng.*, vol. 47, no. 12, pp. 16371–16391, 2022, doi: 10.1007/s13369-022-06925-z.

[21] A. Rauf, N. A. Shah, and T. Botmart, “Hall current and morphological effects on MHD micropolar non - Newtonian tri - hybrid nanofluid flow between two parallel surfaces,” *Sci. Rep.*, no. 0123456789, pp. 1–20, 2022, doi: 10.1038/s41598-022-19625-3.

[22] A. Rehman *et al.*, "Steady Three-Dimensional MHD Mixed Convection Couple Stress Flow of Hybrid Nanofluid with Hall and Ion Slip Effect," vol. 2022, 2022.

[23] U. Hani, M. Ali, and M. S. Alam, "MHD boundary layer micropolar fluid flow over a stretching wedge surface : Thermophoresis and brownian motion effect," *J. Therm. Eng.*, vol. 10, no. 2, pp. 330–349, 2024, doi: 10.18186/thermal.1448609.

[24] F. Abdullahi, D. A. Sani, and M. A. Sani, "Effects of Chemical Reaction and Jeffery Fluid on MHD Unsteady Heat and Mass Transfer Due to the Ramped Temperature," *Int. J. Adv. Eng. Manag.*, vol. 6, no. 10, pp. 368–381, 2024, doi: 10.35629/5252-0610368381.

Cite this Article:

F. Abdullahi, M.A. Sani and M. Mansur, ***"Analysis of Soret and Dufour Effects on Buoyancy driven MHD Heat Mass Transfer Couette Flow under the Influence of Ramped and Isothermal Temperature settings"****, International Journal of Scientific Research in Modern Science and Technology (IJSRMST), ISSN: 2583-7605 (Online), Volume 4, Issue 9, pp. 45-57, September 2025.* ***Journal URL:*** *https://ijsrmst.com/* ***DOI****: https://doi.org/10.59828/ijsrmst.v4i9.367.*